Catching a Moving Target: Comparative Modeling of Flaviviral NS2B-NS3 Reveals Small Molecule Zika Protease Inhibitors

Szymon Pach,[1] Tim M. Sarter,[2] Rafe Yousef,[1] David Schaller,[1] Silke Bergemann,[1] Christoph Arkona,[1] Jörg Rademann,[1] Christoph Nitsche,[2] Gerhard Wolber*[1]

Please insert ORCID IDs here: Szymon Pach 0000-0001-6109-7123, David Schaller: 0000-0002-1881-4518, Jörg Rademann: 0000-0001-6678-3165, Christoph Nitsche: 0000-0002-3704-2699, Gerhard Wolber: 0000-0002-5344-0048

[1] Pharmaceutical and Medicinal Chemistry, Institute of Pharmacy, Freie Universität Berlin, Königin-Luise-Straße 2+4, Berlin 14195, Germany

[2] Research School of Chemistry, Australian National University, Canberra, ACT 2601, Australia

KEYWORDS: Flavivirus, protease, inhibitors, PyRod, 3D pharmacophores, Dynophores.

ABSTRACT: The pivotal role of viral proteases in virus replication has already been successfully exploited in several antiviral drug design campaigns. However, no efficient antivirals are currently available against flaviviral infections. In this study, we present lead-like small molecule inhibitors of the Zika Virus (ZIKV) NS2B-NS3 protease. Since only few non-peptide competitive ligands are known, we take advantage of the high structural similarity with the West Nile Virus (WNV) NS2B-NS3 protease. A comparative modeling approach involving our in-house software *PyRod* was employed to systematically analyze the binding sites and develop molecular dynamics-based 3D pharmacophores for virtual screening. The identified compounds were biochemically characterized revealing low micromolar affinity for both ZIKV and WNV proteases. Their lead-like properties together with rationalized binding modes represent valuable starting points for future lead optimization. Since the NS2B-NS3 protease is highly conserved among flaviviruses, these compounds may also drive the development of pan-flaviviral antiviral drugs.

Flaviviruses cause millions of infections and thousands of fatalities annually.[1] Despite a high medicinal need, no approved anti-flaviviral treatment is currently available.[2] Vaccines preventing infections with frequently prevalent viruses like yellow fever virus,[3] Japanese encephalitis virus,[4] tick-borne encephalitis virus[5] or dengue virus,[6] are approved, but not against emerging species like West Nile virus (WNV) or Zika virus (ZIKV).[2, 7] Due to the high conservation of all flaviviral non-structural (NS) proteins,[8] designing broad-spectrum antivirals is a viable strategy for the treatment of recently emerged species.

Flaviviruses encode for seven NS proteins,[9] whose functions are only understood well for the NS2B-NS3 and NS5.[10] The NS2B-NS3 protease complex is essential for the flaviviral replication cycle by processing the viral polyprotein into functional units of the virion. The non-structural protein 3 (NS3) forms the catalytically active domain of the protease complex.[11] NS2B acts as a co-factor for the protease domain, supporting substrate binding.[12, 13] NS2B-NS3 is a serine protease showing substrate specificity and catalytic triad (S135, H51 and D75, Figure 1) similar to trypsin.[14] This enzyme recognizes dibasic peptide sequences with a cleavage site between an arginine or lysine and amino acids with small sidechains (alanine or serine).[14-17]

NS2B-NS3 represents a promising drug target, since blocking proteases in other virus species, e.g. human immunodeficiency virus[18] or hepatitis C virus,[19] leads to disruption of the replication cycle, which has already yielded several antiviral drugs. Despite high scientific efforts, only few small molecule Zika virus protease ($ZIKV^{Pro}$) inhibitors[20-28] have been reported to date. Several reported non-peptide compounds targeting the active site of the protease show undesirable properties for lead optimization, like instability in aqueous solution[20] or high molecular weight[21, 28] (> 500 Da). As random findings in high-throughput screening campaigns, most active small-molecular competitive inhibitors have poorly characterized binding modes,[21] rendering further development even more challenging. Allosteric inhibitors may lead to fast resistance development.[29] Hence, we strive for the development of drug-like NS2B-NS3 protease inhibitors targeting the substrate-binding site by combining *in-silico* design and biochemical experiments. Our novel, rationally discovered inhibitors with validated binding modes and low molecular weight represent promising starting points for future hit optimization.

Literature research revealed a lack of high-quality bio-activity data for $ZIKV^{Pro}$. Reported competitive ligands show either low potency, high molecular weight or low stability in aqueous solutions.[20, 21, 28] The substrate binding site of WNV protease (WNV^{Pro}) and $ZIKV^{Pro}$ show a sequence identity of 83% (Figure 1) and several non-peptidomimetic ligands for WNV^{Pro} were reported with activity below 50 μM[8] (supporting information Table S1). Hence, WNV^{Pro} was used as a starting point for the identification of novel drug-like $ZIKV^{Pro}$ inhibitors.

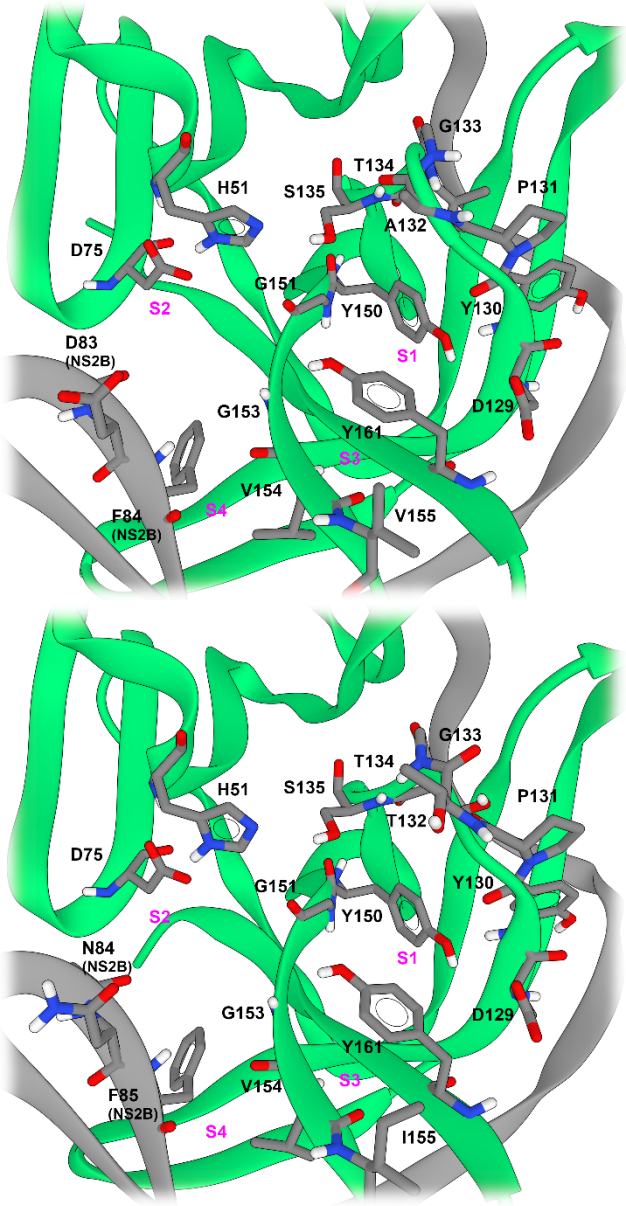

Figure 1. Comparison of ZIKV^{Pro} (top, PDB-ID: 5YOF[20]) and WNV^{Pro} (bottom, PDB-ID: 5IDK[30]) binding pockets. The key-residues are highlighted with black letters and numbers. Pink letters and numbers indicate protease-sub-pockets. Gray backbone- NS2B, green backbone- NS3. This figure was generated using UCSF Chimera 1.13.1.[31]

Substrate binding sites of WNV^{Pro} and ZIKV^{Pro} only differ at three residue positions (Figure 1). The S1 and S2 sub-pockets (Schechter-Berger nomenclature[32]) are highly conserved in flaviviral species[14] and accept lysine and arginine.[14] S3 and S4 sub-pockets show sequence-variability and accept various residues. Both substrate binding sites are highly flexible,[13] hydrophilic and shallow,[33] rendering the NS2B-NS3 protease a challenging target for drug discovery.

In order to address binding pocket flexibility of WNV^{Pro}, we employed our novel application *PyRod*.[34] In this tool, the protein environment of water molecules is analyzed over the course of an MD simulation. Pharmacophoric binding site

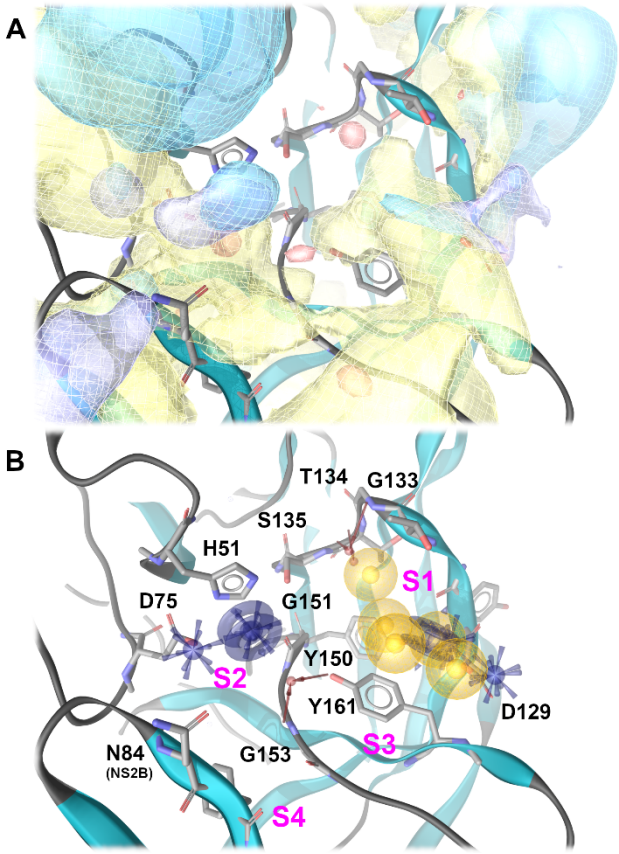

Figure 2. (A) Dynamic molecular interaction fields (dMIFs) and (B) focused (**B1**) 3D-pharmacophore model obtained from WNV^{Pro} MD simulations and *PyRod* analysis. Pink letters and numbers indicate protease sub-pockets. Color code: yellow spheres and clouds- lipophilic contacts, purple rings and blue clouds- aromatic interactions, red arrows and clouds- hydrogen bond acceptors, purple stars and clouds- cationic interactions.

characteristics can subsequently be visualized with dynamic molecular interaction fields (dMIFs, Figure 2A). Features outside the highly conserved S1 and S2 sub-pockets were removed and dMIFs were used to prioritize features inside the binding pocket to generate a focused 3D pharmacophore model consisting of 16 independent features (**B1**, Figure 2B).

Identified cationic interactions exploit contacts in the S1 sub-pocket to D129 and in the S2 sub-pocket to D75 and H51, while aromatic interactions are present facing Y161 and H51 in the S1 and S2 sub-pockets, respectively. Hydrogen bond acceptors are preserved in the essential oxyanion hole (S135, T134, G133) and in the backbone-binding region (G153, Y161). Lipophilic contacts are placed in the conserved regions of the S1 sub-pocket in proximity to Y161 and Y150. The resulting focused pharmacophore was used for combinatorial model library generation with *PyRod*. Since the interaction with residue D129 of NS3 is crucial for substrate recognition,[14-17] we decided that the cationic chemical feature detected by *PyRod* in the S1 sub-pocket (Figure 2B) should be present in each pharmacophore model to enhance the likelihood of finding an active inhibitor. All other pharmacophore features were systematically combined and merged with the cationic feature to generate 3D pharmacophores with three to six independent pharmacophore

features. This procedure resulted in a combinatorial library of 3022 different 3D pharmacophore models. The final pharmacophore ensemble was retrospectively evaluated by screening a collection of 17 small molecular WNV^{Pro} inhibitors reported in the literature[35-39] and 667 decoy molecules derived from the active ligands by the DUD-E server (Database of Useful Decoys: Enhanced).[40]

We compared the obtained early enrichment factors ($EF_{1\%}$) and absolute number of recovered active inhibitors for picking best performing pharmacophores (supporting information Figure S1). The three best performing models (**C1_65**, **C1_397** and **C1_427**, Figure 3) were used for an extensive virtual screening (VS) campaign with more than 7.6 million commercially available compounds. In total 1079 virtual hits were detected (10 for **C1_65**, 712 for **C1_397** and 357 for **C1_427**).

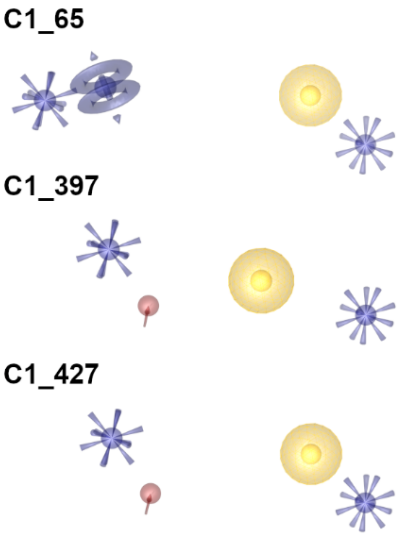

Figure 3. Best performing pharmacophore models obtained from combinatorial model library (yellow spheres- lipophilic contacts, purple rings- aromatic interactions, red arrow- hydrogen bond acceptor, purple star- cationic interaction).

We docked obtained hits into the WNV^{Pro} substrate-binding pocket to explore plausible binding hypotheses. Subsequently, we minimized the energy of docking poses in the binding pocket using LigandScout[41, 42] and scored the ligand conformations based on their fit to the **C1**-pharmacophores (Figure 4).

All compounds were visually inspected to exclude unfavorable virtual hit orientations, such as lipophilic groups pointing towards the solvent, or non-drug like moieties[43] (e.g. quinones) yielding 15 compounds. To ensure that the hits can bind to the highly flexible NS2B-NS3, we performed MD simulations with the best-scoring ligand conformations in complex with the protease. In total, five hits showed no conformational change in the binding pocket throughout 20 ns of MD simulation (Figure 5).

In the next step, we investigated if the five compounds obtained by WNV^{Pro}-modeling can also bind the $ZIKV^{Pro}$ binding pocket. Therefore, we generated a focused 3D pharmacophore (**B2**) for the $ZIKV^{Pro}$ applying *PyRod*, which was compared with the WNV^{Pro} pharmacophore **B1**. Both models showed analogous interaction patterns (Figure 6).

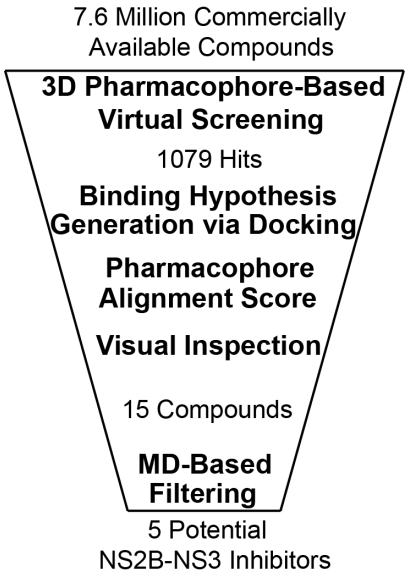

Figure 4. Virtual screening protocol applied for screening of Zika and West Nile virus protease inhibitors.

Moreover, the $ZIKV^{Pro}$ structure exposes aspartic acid at position 83 (homologous to the N84 of WNV^{Pro}) in the NS2B part of the S2 sub-pocket (Figure 1). This polymorphism is proposed to be responsible for higher affinity of $ZIKV^{Pro}$ towards the substrate allowing for salt-bridge formation to lysine or arginine.[44] Due to pharmacophoric properties of selected compounds with conserved cationic interaction in the S2 sub-pocket, we suspected that the hits might be even better $ZIKV^{Pro}$ than WNV^{Pro} inhibitors. After performing docking and MD simulations of the WNV-hits at $ZIKV^{Pro}$, we observed stable binding to the protein, which supported our hypothesis.

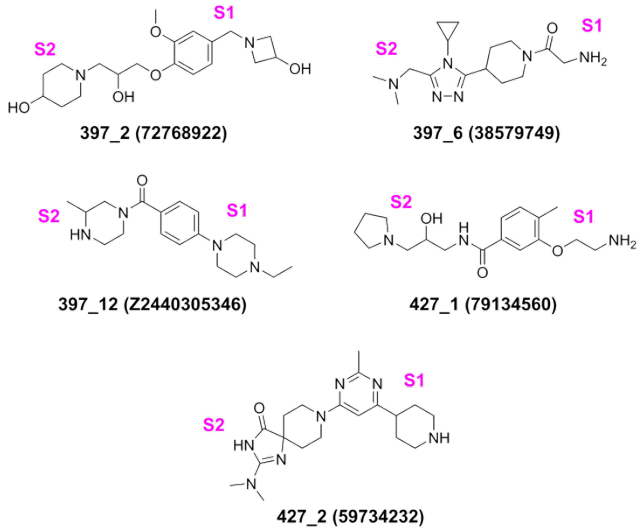

Figure 5. Virtual hits selected for biochemical testing in the $ZIKV^{Pro}$ and WNV^{Pro} assays. Pink letters and numbers indicate assumed arrangement of the compounds towards the protease-sub-pockets.

Table 1. Inhibitory activity of selected hits against ZIKV, WNV, and DENV2 protease.

Compound	ZIKV^{Pro} K_i [µM]	WNV^{Pro} K_i [µM]	DENV2^{Pro} K_i [µM]
397_2	11.5 ± 0.5	7.4 ± 1.3	n.d.
397_6	n.d.	n.d.	n.d.
397_12	n.d.	n.d.	n.d.
427_1	2.3 ± 0.4	25.5 ± 11.8	0.09 ± 0.03
427_2	n.d.	n.d.	n.d.

K_i values were determined for the ligands with inhibition cut-off below 50 µM. n.d.: not determined.

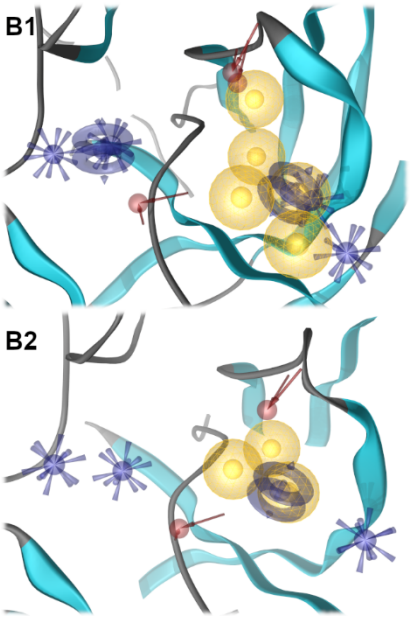

Figure 6. Comparison between focused pharmacophores **B1** (WNV^{Pro} based) and **B2** (ZIKV^{Pro} based) obtained from *PyRod* analysis of MD simulations (yellow spheres- lipophilic contacts, purple rings- aromatic interactions, red arrow- hydrogen bond acceptor, purple star- cationic interaction).

Finally, the five virtual screening hits were evaluated biochemically for inhibition of ZIKV^{Pro} and WNV^{Pro}. Five selected compounds were tested on ZIKV^{Pro} and WNV^{Pro} systems using fluorescence-based assays. Two ligands showed inhibition of both proteases below a 50 µM cut-off. For these compounds, K_i values were determined (Table 1, supporting information Figure S2).

Since molecular modeling was only performed on *R*-enantiomers found in the virtual screening campaign, but the protease assays were carried out with the commercially available racemic mixtures, we assume that the activity of enantiomer-pure compounds would be even higher. Positive testing results encouraged us additionally to evaluate the inhibitory activity of our compounds on closely related Dengue virus 2 (DENV2) protease (for details see Supporting Information). Compound **397_2** showed slightly lower inhibition in the ZIKV^{Pro} than WNV^{Pro} assay, however, as predicted in the same range. Compound **427_1** displayed the highest activity against ZIKV^{Pro} with an unexpected pronounced difference to WNV^{Pro} of one order of magnitude. We surmise that this effect is unrelated to the slightly different pH value in the two the assays (see Supporting Information, page 5). In the next step we established binding hypotheses for the active inhibitors. The suggested binding mode of compound **397_2** is shown in Figure 7. Subsequently, we analyzed why compound **427_1** shows an order of magnitude affinity difference between WNV^{Pro} and ZIKV^{Pro}. To investigate this, we performed 50 ns MD simulations in five replicates and analyzed the trajectories with regard to the ligand-protein interactions using our in-house dynamic pharmacophore analysis method *Dynophore*.[45, 46] We observed recurring comparable interaction patterns indicating two distinct binding modes for the **427_1**-ZIKV^{Pro} complex. The first binding mode is matching our *PyRod* pharmacophore **C1_427** (Figure 7C, Figure **8**A).

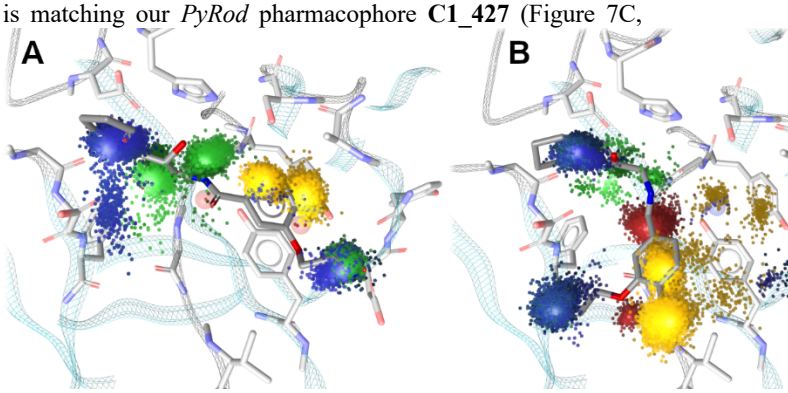

The second one shows preserved interactions in the S2 sub-pocket and additional features between the S3 and S4 sub-pockets (Figure **8**B) introduced by a movement of the aminoethoxyphenyl moiety from the S1 sub-pocket towards D83 of NS2B. The ability to adapt two binding modes could represent an entropic gain resulting in a lower K_i value, even if the crucial S1 sub-pocket is not occupied. Moreover, frequent lipophilic contacts to V155 of the NS3 domain were detected, which potentially contributes to the entropic benefit of the

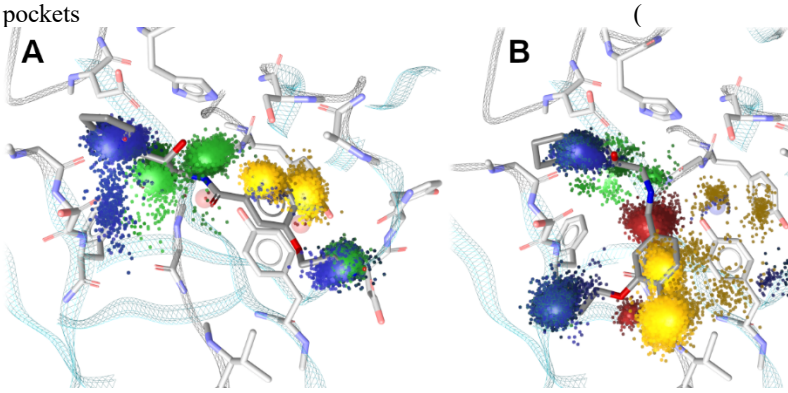

second binding mode. The simulation-analysis of **427_1**-WNV^{Pro} complex shows the same interaction pattern as for ZIKV^{Pro} (Figure 7D, Figure **8**C).

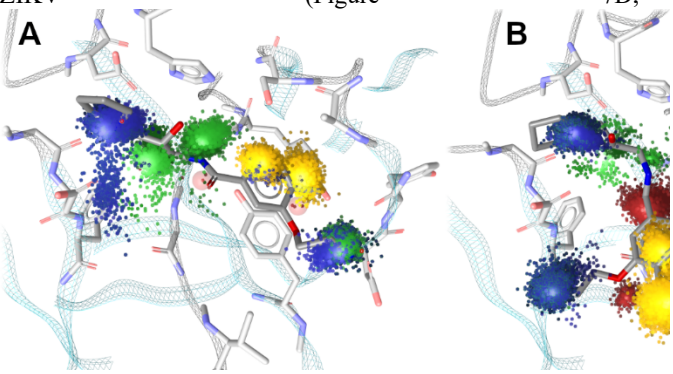

According to the simulation, the second binding mode (dynamic pharmacophore not shown) is less stable and potentially leads to an unbinding event contributing to lower activity of compound **427_1** on the WNV^{Pro}. These findings correspond to the previously hypothesized importance of D83 for ligand binding to the ZIKV^{Pro} as indicated by x-ray crystal structures of peptidomimetic inhibitor-protease complexes.[44, 47] The visual inspection of simulation trajectories of **427_1**-ZIKV^{Pro} complexes shows that the side chain of D83 can adapt two conformations: one pointing towards the S2 sub-pocket and another pointing towards the S3 sub-pocket. The alternative binding hypothesis might be used directly for the optimization of the compound **427_1**. Since WNV^{Pro} expresses an asparagine at position 84 of NS2B, including a cationic moiety pointing towards S3/S4 sub-pockets would not be beneficial, despite reported favorable ionic interaction with D90 in NS2B of WNV^{Pro}.[48] The aminoethoxy-moiety of inhibitor **427_1** is too short to reach this protease region as shown for variety of substrates by Chappell et al.[49] An additional lipophilic moiety and a hydrogen bond donor (as replacement for the amino-moiety of ligand **427_1**) could rather be introduced creating a T-shaped molecule preventing

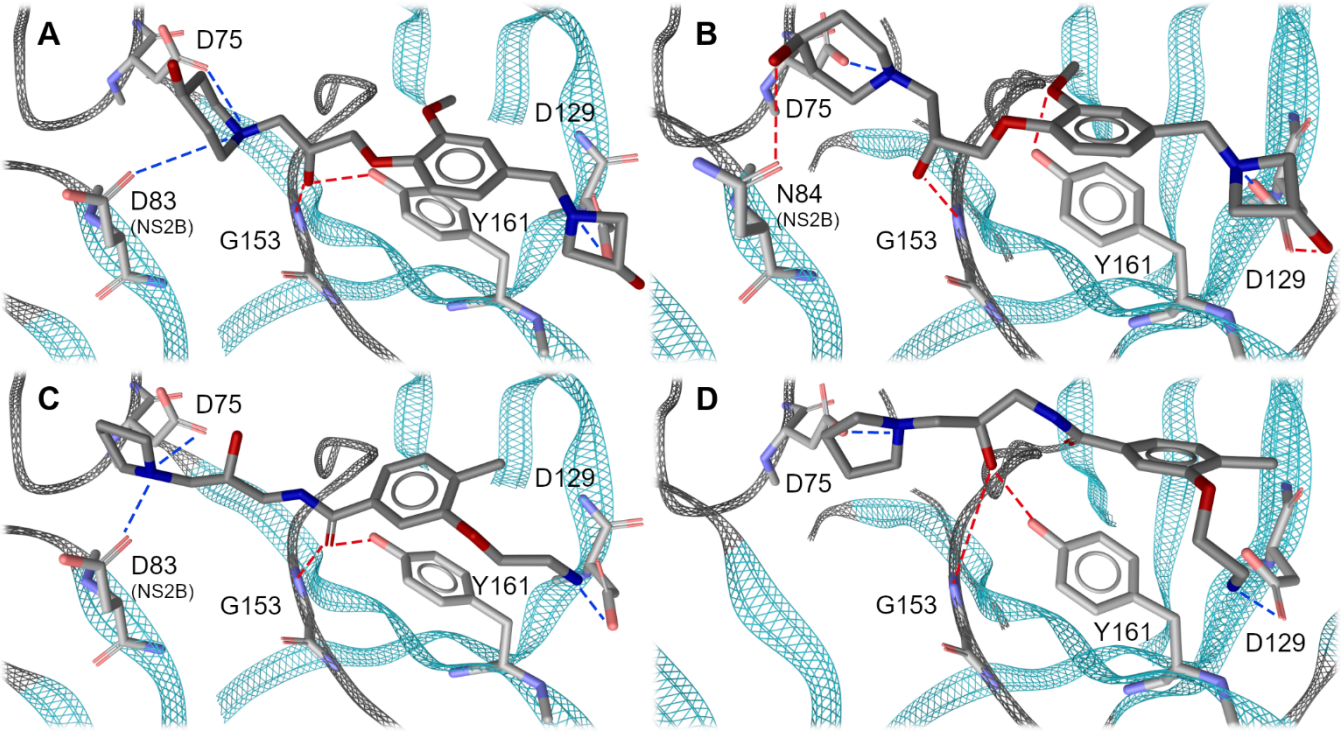

Figure 7. Proposed binding modes for the active inhibitors; compound **397_2** in complex with ZIKV^{Pro} (A) and WNV^{Pro} (B); compound **427_1** in complex with ZIKV^{Pro} (C, according to the *PyRod* pharmacophore) and WNV^{Pro} (D). Color code: blue lines- ionic contacts, red lines- hydrogen bonds.

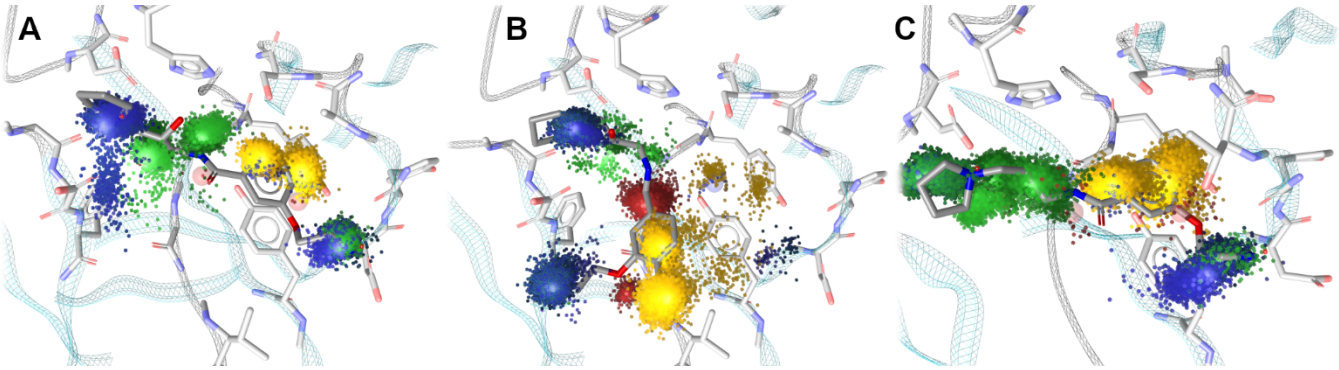

Figure 8. Dynamic pharmacophores generated from MD simulations of compound **427_1**; interaction patterns detected for **427_1**-ZIKV^{Pro} complex (A: dynamic pharmacophore fulfilling the initial binding hypothesis obtained from *PyRod*, B: alternative binding mode supported by the ionic interaction with D83), (C) interaction patterns generated for **427_1**-WNV^{Pro} complex (dynamic pharmacophore fulfilling the initial binding hypothesis obtained from *PyRod*). Color code: yellow points- lipophilic contacts, red and green points- hydrogen bond acceptors and donors, respectively, purple points- cationic interactions.

the ligand from flipping and preserving ionic interactions with crucial D129. We surmise that this ligand design might equalize the activity of inhibitors between WNV^{Pro} and ZIKV^{Pro}We inspected the structures of all ligands tested biochemically to find a suitable descriptor discriminating between active and inactive structures. We put our focus on the flexibility of compounds described as number of rotatable bonds. We surmised that rigid structures cannot adapt to the highly flexible NS2B-NS3 protease. Indeed, the active inhibitors of ZIKV^{Pro} and WNV^{Pro} show more than seven rotatable bonds. This finding indicates that proteases prefer flexible ligands that can adjust to the binding pocket.

In this report, we present two novel, highly active, non-covalent and competitive inhibitors of WNV and ZIKV proteases. To our knowledge, this is the first study performing a successful pharmacophore-based virtual screening campaign against these targets. The identification of the hits was possible by applying the novel software called *PyRod*. It enabled us to overcome challenging features of NS2B-NS3 substrate-binding pockets, such as high flexibility, hydrophilicity and shallowness. The reported compounds represent good starting points for further optimization with established *in silico* binding hypothesis and their drug-like properties, such as low molecular weight and absence of reactive moieties. Moreover, the 3D pharmacophore properties and inhibitory activity of our hits on two different proteases suggests the possibility to develop pan-flaviviral NS2B-NS3 inhibitors.

ASSOCIATED CONTENT

Supporting Information.
This material is available free of charge via the Internet at http://pubs.acs.org.

Computational and experimental methods, and supplementary tables and figures (PDF).

AUTHOR INFORMATION

Corresponding Author

* E-mail: gerhard.wolber@fu-berlin.de

Author Contributions

S.P. designed, conducted and analyzed in-silico experiments, T.S. and C.N. performed and analyzed the ZIKV protease assay and R.Y. the WNV protease assay. C.A. established WNV and DENV2 protease expression and developed WNV and DENV2 assay. S.B. expressed the WNV protease and performed DENV2 protease assay. S.P., T.S., D.S., C.N., J.R. and G.W. wrote the manuscript. J.R., C.N. and G.W. supervised the studies. All authors have given approval to the final version of the manuscript.

ACKNOWLEDGMENT

We acknowledge MS Pharma, Biosupramol (Freie Universität Berlin) for providing us the analytical devices, Lukas Harps and Jan Joseph (Pharmaceutical and Medicinal Chemistry, Institute of Pharmacy, Freie Universität Berlin) for the purity control of tested compounds. C.N. thanks the Australian Research Council for a Discovery Early Career Research Award (DE190100015).

ABBREVIATIONS

DENV2, Dengue virus serotype 2; $EF_{1\%}$, early enrichment factor; MD, molecular dynamics; NS, non-structural protein; VS, virtual screening; WNV, West Nile virus; WNV^{Pro}, West Nile virus protease; ZIKV, Zika virus; ZIKV^{Pro}, Zika virus protease.

REFERENCES

1. Guzman, M. G.; Harris, E., Dengue. *Lancet* **2015,** *385* (9966), 453-65.
2. Chesnut, M.; Munoz, L. S.; Harris, G.; Freeman, D.; Gama, L.; Pardo, C. A.; Pamies, D., In vitro and in silico Models to Study Mosquito-Borne Flavivirus Neuropathogenesis, Prevention, and Treatment. *Front. Cell. Infect. Microbiol.* **2019,** *9*, 223.
3. Theiler, M.; Smith, H. H., The Use of Yellow Fever Virus Modified by in Vitro Cultivation for Human Immunization. *J. Exp. Med.* **1937,** *65* (6), 787-800.
4. Srivastava, A. K.; Putnak, J. R.; Lee, S. H.; Hong, S. P.; Moon, S. B.; Barvir, D. A.; Zhao, B.; Olson, R. A.; Kim, S.-O.; Yoo, W.-D.; Towle, A. C.; Vaughn, D. W.; Innis, B. L.; Eckels, K. H., A purified inactivated Japanese encephalitis virus vaccine made in vero cells. *Vaccine* **2001,** *19* (31), 4557-4565.
5. Zent, O.; Banzhoff, A.; Hilbert, A. K.; Meriste, S.; Służewski, W.; Wittermann, C., Safety, immunogenicity and tolerability of a new pediatric tick-borne encephalitis (TBE) vaccine, free of protein-derived stabilizer. *Vaccine* **2003,** *21* (25-26), 3584-3592.
6. Guy, B.; Barrere, B.; Malinowski, C.; Saville, M.; Teyssou, R.; Lang, J., From research to phase III: preclinical, industrial and

clinical development of the Sanofi Pasteur tetravalent dengue vaccine. *Vaccine* **2011,** *29* (42), 7229-41.

7. Collins, M. H.; Metz, S. W., Progress and Works in Progress: Update on Flavivirus Vaccine Development. *Clin. Ther.* **2017,** *39* (8), 1519-1536.

8. Boldescu, V.; Behnam, M. A. M.; Vasilakis, N.; Klein, C. D., Broad-spectrum agents for flaviviral infections: dengue, Zika and beyond. *Nat. Rev. Drug Discov.* **2017,** *16* (8), 565-586.

9. Simmonds, P.; Becher, P.; Bukh, J.; Gould, E. A.; Meyers, G.; Monath, T.; Muerhoff, S.; Pletnev, A.; Rico-Hesse, R.; Smith, D. B.; Stapleton, J. T.; Ictv Report, C., ICTV Virus Taxonomy Profile: Flaviviridae. *J. Gen. Virol.* **2017,** *98* (1), 2-3.

10. Barrows, N. J.; Campos, R. K.; Liao, K. C.; Prasanth, K. R.; Soto-Acosta, R.; Yeh, S. C.; Schott-Lerner, G.; Pompon, J.; Sessions, O. M.; Bradrick, S. S.; Garcia-Blanco, M. A., Biochemistry and Molecular Biology of Flaviviruses. *Chem. Rev.* **2018,** *118* (8), 4448-4482.

11. Assenberg, R.; Mastrangelo, E.; Walter, T. S.; Verma, A.; Milani, M.; Owens, R. J.; Stuart, D. I.; Grimes, J. M.; Mancini, E. J., Crystal structure of a novel conformational state of the flavivirus NS3 protein: implications for polyprotein processing and viral replication. *J. Virol.* **2009,** *83* (24), 12895-906.

12. Falgout, B.; Pethel, M.; Zhang, Y. M.; Lai, C. J., Both nonstructural proteins NS2B and NS3 are required for the proteolytic processing of dengue virus nonstructural proteins. *J. Virol.* **1991,** *65* (5), 2467-75.

13. Erbel, P.; Schiering, N.; D'Arcy, A.; Renatus, M.; Kroemer, M.; Lim, S. P.; Yin, Z.; Keller, T. H.; Vasudevan, S. G.; Hommel, U., Structural basis for the activation of flaviviral NS3 proteases from dengue and West Nile virus. *Nat. Struct. Mol. Biol.* **2006,** *13* (4), 372-3.

14. Bazan, J. F.; Fletterick, R. J., Detection of a trypsin-like serine protease domain in flaviviruses and pestviruses. *Virology* **1989,** *171* (2), 637-639.

15. Nall, T. A.; Chappell, K. J.; Stoermer, M. J.; Fang, N. X.; Tyndall, J. D.; Young, P. R.; Fairlie, D. P., Enzymatic characterization and homology model of a catalytically active recombinant West Nile virus NS3 protease. *J. Biol. Chem.* **2004,** *279* (47), 48535-42.

16. Chappell, K. J.; Nall, T. A.; Stoermer, M. J.; Fang, N. X.; Tyndall, J. D.; Fairlie, D. P.; Young, P. R., Site-directed mutagenesis and kinetic studies of the West Nile Virus NS3 protease identify key enzyme-substrate interactions. *J. Biol. Chem.* **2005,** *280* (4), 2896-903.

17. Li, J.; Lim, S. P.; Beer, D.; Patel, V.; Wen, D.; Tumanut, C.; Tully, D. C.; Williams, J. A.; Jiricek, J.; Priestle, J. P.; Harris, J. L.; Vasudevan, S. G., Functional profiling of recombinant NS3 proteases from all four serotypes of dengue virus using tetrapeptide and octapeptide substrate libraries. *J. Biol. Chem.* **2005,** *280* (31), 28766-74.

18. Ghosh, A. K.; Osswald, H. L.; Prato, G., Recent Progress in the Development of HIV-1 Protease Inhibitors for the Treatment of HIV/AIDS. *J. Med. Chem.* **2016,** *59* (11), 5172-208.

19. Asselah, T.; Boyer, N.; Saadoun, D.; Martinot-Peignoux, M.; Marcellin, P., Direct-acting antivirals for the treatment of hepatitis C virus infection: optimizing current IFN-free treatment and future perspectives. *Liver Int.* **2016,** *36 Suppl 1*, 47-57.

20. Li, Y.; Zhang, Z.; Phoo, W. W.; Loh, Y. R.; Li, R.; Yang, H. Y.; Jansson, A. E.; Hill, J.; Keller, T. H.; Nacro, K.; Luo, D.; Kang, C., Structural Insights into the Inhibition of Zika Virus NS2B-NS3 Protease by a Small-Molecule Inhibitor. *Structure* **2018,** *26* (4), 555-564 e3.

21. Lee, H.; Ren, J.; Nocadello, S.; Rice, A. J.; Ojeda, I.; Light, S.; Minasov, G.; Vargas, J.; Nagarathnam, D.; Anderson, W. F.; Johnson, M. E., Identification of novel small molecule inhibitors against NS2B/NS3 serine protease from Zika virus. *Antiviral Res.* **2017,** *139*, 49-58.

22. Yao, Y.; Huo, T.; Lin, Y. L.; Nie, S.; Wu, F.; Hua, Y.; Wu, J.; Kneubehl, A. R.; Vogt, M. B.; Rico-Hesse, R.; Song, Y., Discovery, X-ray Crystallography and Antiviral Activity of Allosteric Inhibitors of Flavivirus NS2B-NS3 Protease. *J. Am. Chem. Soc.* **2019,** *141* (17), 6832-6836.

23. Rassias, G.; Zogali, V.; Swarbrick, C. M. D.; Ki Chan, K. W.; Chan, S. A.; Gwee, C. P.; Wang, S.; Kaplanai, E.; Canko, A.; Kiousis, D.; Lescar, J.; Luo, D.; Matsoukas, M. T.; Vasudevan, S. G., Cell-active carbazole derivatives as inhibitors of the zika virus protease. *Eur. J. Med. Chem.* **2019,** *180*, 536-545.

24. Millies, B.; von Hammerstein, F.; Gellert, A.; Hammerschmidt, S.; Barthels, F.; Goppel, U.; Immerheiser, M.; Elgner, F.; Jung, N.; Basic, M.; Kersten, C.; Kiefer, W.; Bodem, J.; Hildt, E.; Windbergs, M.; Hellmich, U. A.; Schirmeister, T., Proline-Based Allosteric Inhibitors of Zika and Dengue Virus NS2B/NS3 Proteases. *J. Med. Chem.* **2019,** *62* (24), 11359-11382.

25. Brecher, M.; Li, Z.; Liu, B.; Zhang, J.; Koetzner, C. A.; Alifarag, A.; Jones, S. A.; Lin, Q.; Kramer, L. D.; Li, H., A conformational switch high-throughput screening assay and allosteric inhibition of the flavivirus NS2B-NS3 protease. *PLoS Pathog.* **2017,** *13* (5), e1006411.

26. Shiryaev, S. A.; Farhy, C.; Pinto, A.; Huang, C. T.; Simonetti, N.; Elong Ngono, A.; Dewing, A.; Shresta, S.; Pinkerton, A. B.; Cieplak, P.; Strongin, A. Y.; Terskikh, A. V., Characterization of the Zika virus two-component NS2B-NS3 protease and structure-assisted identification of allosteric small-molecule antagonists. *Antiviral Res.* **2017,** *143*, 218-229.

27. Roy, A.; Lim, L.; Srivastava, S.; Lu, Y.; Song, J., Solution conformations of Zika NS2B-NS3pro and its inhibition by natural products from edible plants. *PLoS One* **2017,** *12* (7), e0180632.

28. Yuan, S.; Chan, J. F.; den-Haan, H.; Chik, K. K.; Zhang, A. J.; Chan, C. C.; Poon, V. K.; Yip, C. C.; Mak, W. W.; Zhu, Z.; Zou, Z.; Tee, K. M.; Cai, J. P.; Chan, K. H.; de la Pena, J.; Perez-Sanchez, H.; Ceron-Carrasco, J. P.; Yuen, K. Y., Structure-based discovery of clinically approved drugs as Zika virus NS2B-NS3 protease inhibitors that potently inhibit Zika virus infection in vitro and in vivo. *Antiviral Res.* **2017,** *145*, 33-43.

29. Kurt Yilmaz, N.; Swanstrom, R.; Schiffer, C. A., Improving Viral Protease Inhibitors to Counter Drug Resistance. *Trends Microbiol.* **2016,** *24* (7), 547-557.

30. Nitsche, C.; Zhang, L.; Weigel, L. F.; Schilz, J.; Graf, D.; Bartenschlager, R.; Hilgenfeld, R.; Klein, C. D., Peptide-Boronic Acid Inhibitors of Flaviviral Proteases: Medicinal Chemistry and Structural Biology. *J. Med. Chem.* **2017,** *60* (1), 511-516.

31. Pettersen, E. F.; Goddard, T. D.; Huang, C. C.; Couch, G. S.; Greenblatt, D. M.; Meng, E. C.; Ferrin, T. E., UCSF Chimera--a visualization system for exploratory research and analysis. *J. Comput. Chem.* **2004,** *25* (13), 1605-12.

32. Berger, A.; Schechter, I., Mapping the active site of papain with the aid of peptide substrates and inhibitors. *Philos. Trans. R. Soc. Lond. B. Biol. Sci.* **1970,** *257* (813), 249-64.

33. Nitsche, C., Proteases from dengue, West Nile and Zika viruses as drug targets. *Biophys. Rev.* **2019,** *11* (2), 157-165.

34. Schaller, D.; Pach, S.; Wolber, G., PyRod: Tracing Water Molecules in Molecular Dynamics Simulations. *J. Chem. Inf. Model.* **2019,** *59* (6), 2818-2829.

35. Ekonomiuk, D.; Su, X. C.; Ozawa, K.; Bodenreider, C.; Lim, S. P.; Otting, G.; Huang, D.; Caflisch, A., Flaviviral protease inhibitors identified by fragment-based library docking into a structure generated by molecular dynamics. *J. Med. Chem.* **2009,** *52* (15), 4860-8.

36. Ekonomiuk, D.; Su, X. C.; Ozawa, K.; Bodenreider, C.; Lim, S. P.; Yin, Z.; Keller, T. H.; Beer, D.; Patel, V.; Otting, G.; Caflisch, A.; Huang, D., Discovery of a non-peptidic inhibitor of west nile virus NS3 protease by high-throughput docking. *PLoS Negl. Trop. Dis.* **2009,** *3* (1), e356.

37. Bodenreider, C.; Beer, D.; Keller, T. H.; Sonntag, S.; Wen, D.; Yap, L.; Yau, Y. H.; Shochat, S. G.; Huang, D.; Zhou, T.; Caflisch, A.; Su, X. C.; Ozawa, K.; Otting, G.; Vasudevan, S. G.; Lescar, J.; Lim, S. P., A fluorescence quenching assay to discriminate between specific and nonspecific inhibitors of dengue virus protease. *Anal. Biochem.* **2009,** *395* (2), 195-204.

38. Ganesh, V. K.; Muller, N.; Judge, K.; Luan, C. H.; Padmanabhan, R.; Murthy, K. H., Identification and characterization of nonsubstrate based inhibitors of the essential dengue and West Nile virus proteases. *Bioorg. Med. Chem.* **2005,** *13* (1), 257-64.

39. Cregar-Hernandez, L.; Jiao, G. S.; Johnson, A. T.; Lehrer, A. T.; Wong, T. A.; Margosiak, S. A., Small molecule pan-dengue and West Nile virus NS3 protease inhibitors. *Antivir. Chem. Chemother.* **2011,** *21* (5), 209-17.

40. Mysinger, M. M.; Carchia, M.; Irwin, J. J.; Shoichet, B. K., Directory of useful decoys, enhanced (DUD-E): better ligands and decoys for better benchmarking. *J. Med. Chem.* **2012,** *55* (14), 6582-94.

41. Wolber, G.; Dornhofer, A. A.; Langer, T., Efficient overlay of small organic molecules using 3D pharmacophores. *J. Comput. Aided Mol. Des.* **2006,** *20* (12), 773-88.

42. Wolber, G.; Langer, T., LigandScout: 3-D pharmacophores derived from protein-bound ligands and their use as virtual screening filters. *J. Chem. Inf. Model.* **2005,** *45* (1), 160-9.

43. Baell, J. B.; Holloway, G. A., New substructure filters for removal of pan assay interference compounds (PAINS) from screening libraries and for their exclusion in bioassays. *J. Med. Chem.* **2010,** *53* (7), 2719-40.

44. Lei, J.; Hansen, G.; Nitsche, C.; Klein, C. D.; Zhang, L.; Hilgenfeld, R., Crystal structure of Zika virus NS2B-NS3 protease in complex with a boronate inhibitor. *Science* **2016,** *353* (6298), 503-5.

45. Bock, A.; Bermudez, M.; Krebs, F.; Matera, C.; Chirinda, B.; Sydow, D.; Dallanoce, C.; Holzgrabe, U.; De Amici, M.; Lohse, M. J.; Wolber, G.; Mohr, K., Ligand Binding Ensembles Determine Graded Agonist Efficacies at a G Protein-coupled Receptor. *J. Biol. Chem.* **2016,** *291* (31), 16375-89.

46. Mortier, J.; Prevost, J. R. C.; Sydow, D.; Teuchert, S.; Omieczynski, C.; Bermudez, M.; Frederick, R.; Wolber, G., Arginase Structure and Inhibition: Catalytic Site Plasticity Reveals New Modulation Possibilities. *Sci. Rep.* **2017,** *7* (1), 13616.

47. Li, Y.; Zhang, Z.; Phoo, W. W.; Loh, Y. R.; Wang, W.; Liu, S.; Chen, M. W.; Hung, A. W.; Keller, T. H.; Luo, D.; Kang, C., Structural Dynamics of Zika Virus NS2B-NS3 Protease Binding to Dipeptide Inhibitors. *Structure* **2017,** *25* (8), 1242-1250 e3.

48. Lim, H. A.; Ang, M. J.; Joy, J.; Poulsen, A.; Wu, W.; Ching, S. C.; Hill, J.; Chia, C. S., Novel agmatine dipeptide inhibitors against the West Nile virus NS2B/NS3 protease: a P3 and N-cap optimization study. *Eur. J. Med. Chem.* **2013,** *62*, 199-205.

49. Chappell, K. J.; Stoermer, M. J.; Fairlie, D. P.; Young, P. R., Insights to substrate binding and processing by West Nile Virus NS3 protease through combined modeling, protease mutagenesis, and kinetic studies. *J. Biol. Chem.* **2006,** *281* (50), 38448-58.